Comparison Between Rectangular and Cylindrical Continuous Ohmic Heating Modelling

[1]Elzubier Ahmed Salih & [2]Sergey Spotar

[1]Department of Food Engineering, Faculty of Engineering and Technology, University of Gezira, Sudan
[2]Department Of Chemical Engineering, Faculty of Engineering, Nottingham University, Malaysia

ABSTRACT

Two-dimensional models is developed for collinear cylindrical continuous ohmic heating cell (3-ring electrode inserted in cylindrical column one at the middle and the other two at extremities) and rectangular continuous ohmic heating (two parallel plate electrode inserted along 0.5m long) to simulate the Electric field distribution, temperature and velocity profiles during continuous ohmic heating of non-Newtonian power law liquid food (Guava juice) using computational fluid dynamic (CFD) codes using A user defined functions (UDFs) which is employed in original flat pattern FLUENT 6.1 for electric field equation. The simulation was carried with and without buoyancy driven force effects. The buoyancy effects show significance effect in both colliner and parallel plate electrodes configuration ohmic heating in this study, the parallel plate electrode configuration (transverse electric fields) ohmic heating show uniform temperature distribution than the collinear one. The computations domain used for the cylindrical heating cell (with diameter of 0.05m and height of 0.50m, and have three electrodes, each electrode have width of 0.02m and the distances between electrode is 0.22m) and the rectangular heating cell (with length of 0.2m, width of 0.04m and height 0.6m, the plate electrode is 0.2m×0.04m×0.6m inserted along the wall) . In the rectangular ohmic heating the flow behavior measurement was used to validate the CFD simulation using water in the temperature range 30-40 ^{0}C and in the cylindrical ohmic heating for guava juice in temperature range 30-90^{0}C.

Key word: ohmic heating, mixed convection, comparison, cylindrical and rectangular ohmic heating cell.

INTRODUCTION

Ohmic heating is defined as a process where electric currents are passed through foods with the main purpose of heating them by internal energy generation (de Alwis and Fryer, 1990). It has recently gained new interest because the products obtained are of clearly superior quality than those processed by conventional technologies. This is mainly due to its ability to heat materials rapidly and uniformly leading to a less aggressive thermal treatment (which, otherwise, often leads to over processed volumes).

Ohmic heating can be considered a High Temperature Short Time (HTST) aseptic process. The potential applications of this technique in food industry are very wide and include e.g. blanching, evaporation, dehydration, fermentation and pasteurization. Especially interesting is the application of this technique to foods containing solid

Corresponding author E mail elzubiersalih@yahoo.com

particles and/or being viscous fluids (e.g. fruit purees and fruit pulps).

The most critical property affecting ohmic heating rate is food electrical conductivity. Food electrical conductivity is affected by a large number of parameters such as temperature, ionic strength, free water material microstructure (Lima and Sastry, 1999)

In a collinear ohmic heating device, the electric field and current flux are parallel to the flow, and in transverse ohmic heating, the applied electric field and current flux are at right angles to the mass flow of the fluid. Quite a few scientific and technical works have been dedicated to the heat treatment of homogenous food fluids by ohmic heating technology (Marcotte. 1999; Ould Elmuktar, et al., 1993).

The objective of this study was

considers the design To develop a fully three-dimensional non-symmetric model which 1.

to verify model predictions at a set of of heating cell and location of electrodes, and

will provide key information on the pasteurization and cook value representative locations. This

heatingcell, electrode (Ye, et al.,2004).This method may be used in the design of

temperatures for minimizing cold spots during the configurations, process time and

process (Abdul Ghani, et al., 2002). pasteurization

yield the most To optimize electrode configurations in a cylindrical ring shape to 2.

continuous systems and to compare uniform yet rapid heating thermal profiles in

transverse electric field ohmic heating. between collinear and

MATERIAL AND METHOD

1- Materials

Pink guava juices and water

2- Method

2.1. Simulation technique

Advanced CFD technology allows handling of complex geometries, while capturing the complex physics involved in laminar and turbulent flows. A CFD mathematical model simulates problems arising in chemical processes, offering an easy-to-use interface with powerful graphics

and optimization procedures. FLUENT software package version 6.1 was used to solve mass, momentum, energy equations for 2D models of laminar Non-Newtonian (guava juice) using continuous ohmic heating unit to perform pasteurization process. Structured mesh was generated using GAMBIT 2.0. Grids created with gambit were then read in FLUENT.
The grid was checked by FLUENT to make sure that all the volumes created are positive. Operating conditions and boundary conditions were specified, as well as the properties of the different fluids present in the system. For a better control of the solution, different algorithms were selected and the level of convergence desired by the user was selected. Before starting to iterate, properties of the flow field such as velocity, temperature, and viscosity parameters were initialized from a specified boundary. The Segregated solver was chosen as the numerical solution method in FLUENT. This approach segregates the governing equations and solves them sequentially. In addition, the governing equations are non-linear, which requires several iterations of the solution loop to be performed. Schematic ohmic heating cell of collinear electrodes of 0.5m length. This shown in Figure 1. From the guava juice and soymilk property assumptions, the solver flow regime was selected as incompressible.
The solver flow type was set as laminar. Since there were no time-dependent terms, the simulation type was chosen as steady-state.

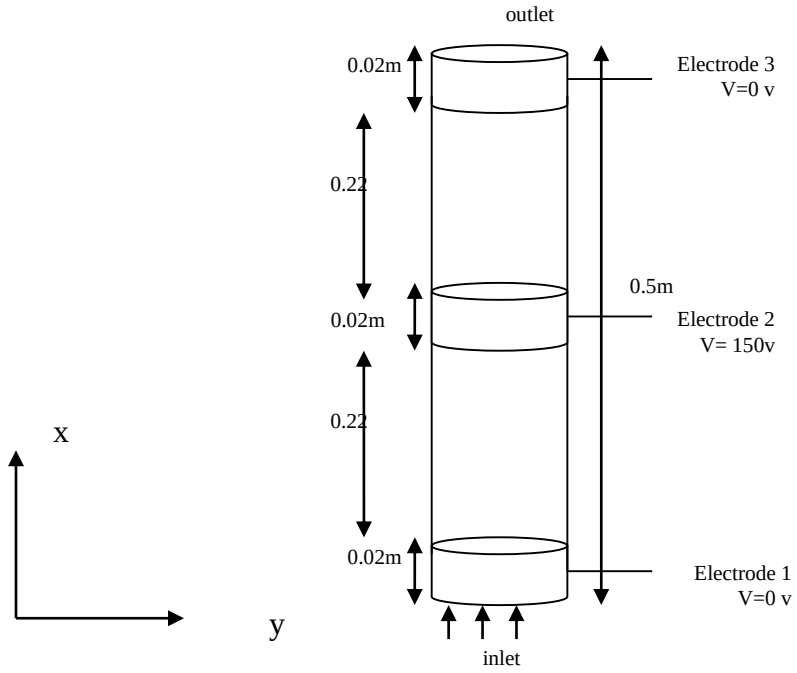

Figure **Error! No text of specified style in document.**

Schematic ohmic heating cell of collinear electrodes of 0.5m length

Table **Error! No text of specified style in document.**

The parameters of guava juice used in simulation

parameters	Guava juice
Consistency index	K = 0.117 Pa s^n
Flow behavior index	n = 0.5978
Density	ρ = 1041.1 – 0.6896 T kg/m^3
Thermal conductivity	k= 0.4401 +0.0039 T J/m ^{0}C
Specific heat	C_p = 4035.7 + 17.935 T J/kg ^{0}C
Electrical conductivity	σ = 0.0038 T + 0.0642 s/m
viscosity	0.013Pa s
Velocity	0.003m/s
β	0.00051
σ_0	0.00383s/m

A user-defined function, or UDF, is a programmed function that can be dynamically loaded with the FLUENT solver to enhance the standard features of the code. UDFs are written in the C or C++ programming language. They are defined using 'DEFINE macros' that are supplied by Fluent Inc. In this work the user defined function codes were written for parabolic inlet velocity for 2D and 3D model.

For every iteration, the residual for continuity, components of velocity, energy parameters is calculated. The residual for each variable is the difference between the values calculated at iteration N-1 and. FLUENT plots the evolution of the residuals vs iteration number. As long as the residuals are greater than the convergence criterions the code keeps iterating. The convergence criterions can be decreased to obtain more accurate results but it also increases dramatically the CPU time. In this study the convergence criterions were taken as 10^{-3} for continuity, momentum and 10^{-6} for electric field (UDS) and energy.

2.2. Numerical simulation using cylindrical ohmic heating

The simulation was done using 2D-axi symmetric continuous ohmic heating of 0.5m length (see Figure 1.)

2. 2.1. Assumptions

To simplify the problem, the following assumptions were made

1. Steady, laminar and 2D;
2. Heat generation due to viscous dissipation is negligible;
3. Incompressible fluid;
4. No energy dissipation in thermal boundary layer;

5. Small axial conduction relative to radial conduction;
6.There is no heat loss to the surroundings and that the tube is insulated;
7.The wall of the heating cell was electrically insulated implies that no voltage gradient across the wall;
temperature;
8. Boussinesq approximation is valid, i.e., the density difference, which causes the flow, has a linear relationship with

9. Specific heat Cp, thermal conductivity k, are temperature Dependent for soymilk
10. no-slip condition at the inside wall of the heating cell; physical properties are

11. The center of the heating cell is a point of symmetry;

12. The fluid rheological properties (guava juice) and thermo

conductivity of guava juice is constant; Temperature dependent except the thermal

2.2.2 Governing equations

The notation of FLUENT is adapted here.

Continuity equation

$$\frac{1}{r}\frac{\partial}{\partial r}(r\rho v_r)+\frac{\partial}{\partial x}(\rho v_x)=0 \qquad (1)$$

Where v is the fluid velocity;

Momentum

The general equation for fluid flow can be found in standard books (Bird et al., 1976). Considering a vertical cylindrical heating cell in which electrodes are inserted, the momentum equation for the vertical velocity v_x in cylindrical coordinates is expressed by:

$$\rho\left(\frac{\partial v_x}{\partial t}+v_r\frac{\partial v_x}{\partial r}+v_x\frac{\partial v_x}{\partial x}\right)=-\frac{\partial p}{\partial x}+\rho_0\left[1+\beta(T-T_0)\right]g_x+\frac{1}{r}\frac{\partial}{\partial r}\left(\mu_a r\frac{\partial v_x}{\partial r}\right)+\frac{\partial}{\partial x}\left(\mu_a\frac{\partial v_x}{\partial x}\right) \qquad (2)$$

$$\text{Where } \mu_a = K\left(-\frac{\partial v_r}{\partial x}\right)^{n-1} \qquad (3)$$

The component of the velocity in the θ direction is assumed negligible. The Boussinesq approximation in which the density is vary with temperature in the buoyancy term:

$$\rho=\rho_0\left[1+\beta(T-T_0)\right] \qquad (4)$$ The radial direction v_r is zero (fully developed) and the flow is steady stte then $\frac{\partial v_x}{\partial t}=0$, and $\frac{\partial v_x}{\partial x}=0$ because is very small

Then the equation is simplified

$$\rho\left(v_x\frac{\partial v_x}{\partial x}\right)=-\frac{\partial p}{\partial x}+\rho_0\left[1+\beta(T-T_0)\right]g_x+\frac{1}{r}\frac{\partial}{\partial r}\left(\mu_a r\frac{\partial v_x}{\partial r}\right) \quad (5)$$

Radial equation

$$\rho\left(\frac{\partial v_r}{\partial t}+v_r\frac{\partial v_r}{\partial r}+v_x\frac{\partial v_r}{\partial x}\right)=-\frac{\partial p}{\partial r}+\left[\frac{\partial}{\partial r}\left(\frac{1}{r}\frac{\partial}{\partial r}\left(\mu_a r v_r\right)\right)+\frac{\partial^2 v_r}{\partial x^2}\right] \quad (6)$$

$$\mu_a=k\left(-\frac{\partial v_r}{\partial x}\right)^{n-1} \quad (7)$$

The velocity in the x-direction is a function of the r position and will be determined by the flow regime, which is laminar in nature. The flow behavior is also dependent on the viscosity of the fluid. Assuming a fully developed flow, the 2D velocity for a power law non-Newtonian fluid at the inlet was computed from the following: (Bird, Stewart and Lightfoot, (1976)):

$$v_z(0,r,)=\frac{Vo}{\pi R^2}\left[\frac{3n+1}{n+1}\right]\left[1-\left(\frac{r}{R^2}\right)^{\frac{n-1}{n}}\right] \quad (8)$$

Vo is the volumetric flow rate, n is the flow behavior index, and z, r, are coordinate.
Power law models was used to describe the flow behavior of guava juice solution as a function of shear stress and shear rate

$$\tau=k\gamma^n \quad (9)$$

where τ is the shear stress, k consistency coefficient, n flow behavior index and γ is the shear rate. The viscosity, which changes with shear rate, is termed apparent viscosity η_a. The term apparent implies a Newtonian type of measurement to a non-Newtonian system and is described by equation 10.

$$\eta_a=\frac{\tau}{\gamma}=k\gamma^{n-1} \quad (10)$$

where η_a is the apparent viscosity of the fluid
Both the consistency coefficient index (k) and flow behavior index (n) are temperature dependent. For free convection, the temperature driving force was included in a Grash of number

$$Gr=\frac{\rho^2 g D^3 \Delta T\beta}{\mu^2} \quad (11)$$

Where Gr is dimensionless Grashof number
Considering the effect of electrical field, a modified Grashof number was used. The electric Grashof number is defined: (Kronig and Ahsmann (1949),

$$\mathrm{Gr}_{El}=\frac{\rho^2\beta\Delta T D^2 E^2 b}{\mu^2} \quad (12)$$

The thermal behavior is based on the energy balance. It includes convection, conduction and heat generation. Given by Equation 11

The energy equation:

The axi symmetric problem can be expressed as

$$\rho C_p\left(v_r\frac{\partial T}{\partial r}+v_x\frac{\partial T}{\partial x}\right)=\frac{1}{r}\frac{\partial}{\partial r}\left(kr\frac{\partial T}{\partial r}\right)-\frac{\partial}{\partial x}\left(k\frac{\partial T}{\partial x}\right)+Q \qquad (13)$$

Electric field distribution equation

The Laplace equation for electric field distribution was solved in the whole fluid at steady state to find the heat generation rate: As proposed by de Alwis et al. (1990),

$$\nabla\left(\sigma_f\nabla V\right)=0 \qquad (14)$$

Where the electrical conductivity is temperature dependant. The value of σ increases with temperature as follows:

$$\sigma_f=\sigma_{30}+m_T\left(T-30\right) \qquad (15)$$

so, the solution of the Laplace equation is dependent on the temperature distribution in the tube. In cylindrical coordinates, the electric field distribution of the spacing tube between the two electrodes can be calculated as:

$$\frac{\partial}{\partial x}\left(\sigma_f\frac{\partial V}{\partial x}\right)+\frac{1}{r}\frac{\partial}{\partial r}\left(r\sigma_f\frac{\partial V}{\partial r}\right)=0 \qquad (16)$$

The general volumetric heating rate is as follows

$$Q_f=\sigma_f\left(\nabla V\cdot\nabla V\right)=\left|\nabla V\right|^2\sigma_f \qquad (17)$$

and the heat generation = heating rate divided by the volume of the fluid

2.2.3. Boundary conditions

The boundary conditions are:

At the axis or Y=0 (center of the pipe) $\frac{\partial T}{\partial y}=0,\frac{\partial v_x}{\partial y}=0,\frac{\partial V}{\partial y}=0$, $v_{yr}=0,v_z=0$

At the wall or Y=Y, $\frac{\partial T}{\partial y}=0,\frac{\partial v_x}{\partial y}=0,\frac{\partial V}{\partial y}=0$, $\boldsymbol{v_y=0, v_x=0}$

And at the electrode, the high value is at the middle and 0 volt at both extremities. The other wall is insulated.

At the inlet or x=0, $T=T_{in}$, $v_y=0$

Initial conditions

V= 0 volt, v_m= 0.003m/s and velocity for non-Newtonian fluid:

$$v_x = v_x(0,y) = \frac{G}{\pi R^2}\left[\frac{3n+1}{n+1}\right]\left[1-\left(\frac{y}{R}\right)^{\frac{n+1}{n}}\right]$$

And for Newtonian fluid:

$$v_x = v_x(0,y) = \frac{G}{\pi R^2}\left[1-\left(\frac{y}{R}\right)^2\right] \qquad T_i = 30^0C,$$

2.3. Rectangular geometry ohmic heating:

The simulation was done for water is the set up as shown in figure 2.

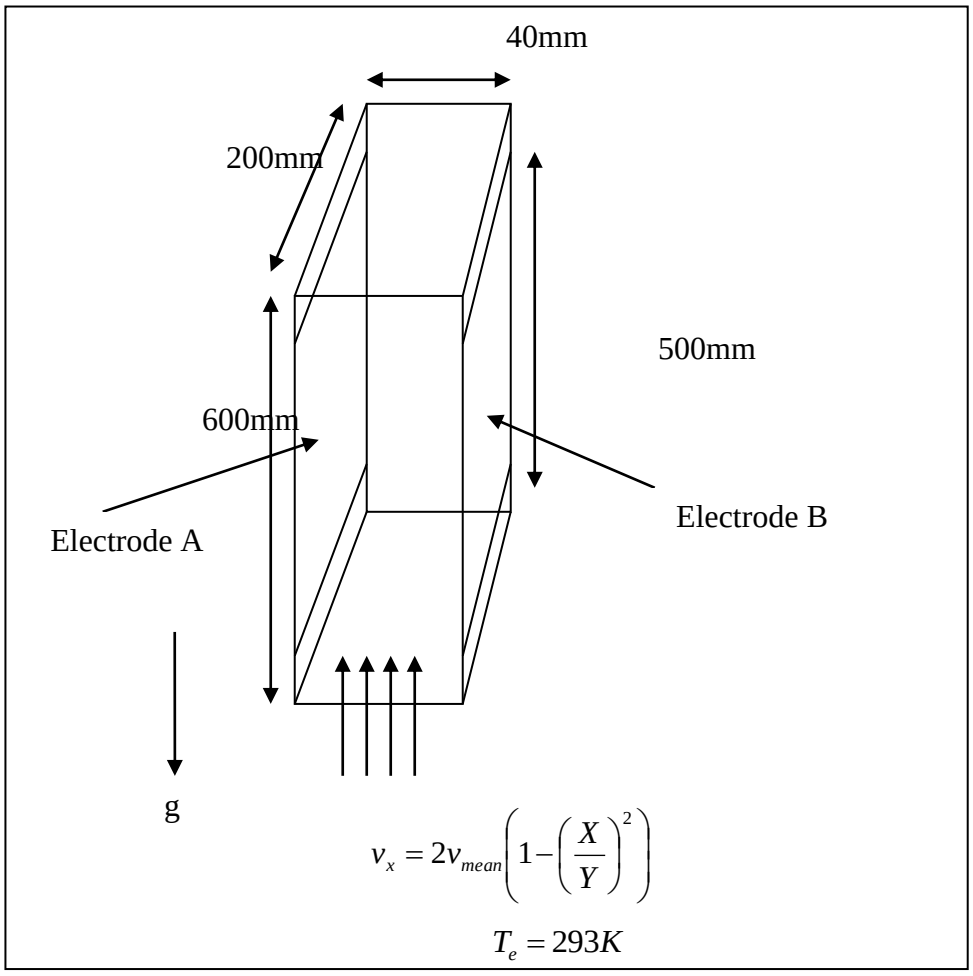

Figure 2 Flow Geometry and the boundary conditions for rectangular channel ohmic heating

The physical properties of the working fluid for the rectangular channel are as given in Table 2.

Table 2 The physical properties of the working fluid (water)

ρ_{inlt}	996.84 kg/m^3
ρ_{out}	994.25 kg/m^3
C_p	4185 J/kgK
μ	0.0008843 kg/ms
k	0.61W/mK
σ	0.0275 S/m

The mean velocity (V_m= 0.0073m/s), the voltage applied (V= 242.5 volts) and the temperature difference (T_{in} - T_{out}) = 10.46 K) were taken from Ould El Moctar (1996). The density is assumed to vary by a linear dependence on temperature.
To solve the governing equations the following assumptions is used

2.3.1. Assumptions:

1- Constant properties (μ, ρ, k, C_p) except for the variation in density that drives the flow.
2- The boussinesq equation is important(free convection)
3- Steady state
4- Viscous dissipation is negligible in the energy equation
5- The flow is two dimensional and fully developed
6- Fluid inter the channel at constant temperature.

2.3.2. The governing equations: For the rectangular coordinates (x, y)

Continuity

$$\frac{\partial v_x}{\partial x}+\frac{\partial v_y}{\partial y}=0 \qquad (18)$$

Momentum

Momentum for vertical flow (axial direction)
Because the flow is fully developed and the conventional flow is bigger than the radial convection so we can consider the flow is one-dimensional flow, in the vertical direction only.

$$\rho\left(v_x\frac{\partial v_x}{\partial x}+v_y\frac{\partial v_x}{\partial y}\right)=-\frac{\partial p}{\partial x}+\eta\left[\frac{\partial^2 v_x}{\partial x^2}+\frac{\partial^2 v_x}{\partial y^2}\right]+\rho[1-\beta(T-T_0)]g \qquad (19)$$

Momentum for the radial direction:

$$(20)\quad \rho\left(v_x\frac{\partial v_y}{\partial x}+v_y\frac{\partial v_y}{\partial y}\right)=-\frac{\partial p}{\partial y}+\eta\left[\frac{\partial^2 v_y}{\partial x^2}+\frac{\partial^2 v_y}{\partial y^2}\right]$$

Energy equation:

$$\rho C_p\left[v_x\frac{\partial T}{\partial x}+v_y\frac{\partial T}{\partial y}\right]=k\left[\frac{\partial^2 T}{\partial x^2}+\frac{\partial^2 T}{\partial y^2}\right]+Q \qquad (21)$$

Where Q is the heat generation per unit volume

Electric filed equation:

$$\left(\sigma_f \frac{\partial V}{\partial x} + \sigma_f \frac{\partial V}{\partial y}\right) = 0 \qquad (22)$$

2.4. Solution convergence

The governing equations are solved using the commercially available Computational Fluid Dynamics (CFD) software Fluent 6.1 and the computer system intel/2R, 2.85 GHz, and 3GB Ram machine running window 2002 professional was used in the simulation. The mesh for 2D model was adapted at different times for both geometry until stable solutions (grid independent solution) was achieved.

RESULTS AND DISCUSSION

1. The cylindrical ohmic heating:

There was uniform temperature distribution found in the heating cell as result of variations near the heating cell wall and that flowing near the center of the heating cell. As the volumetric heating rate was increased, both the flow and temperature distributions began to change. The velocity distribution becomes flatter in the central zone, rising to a maximum value before dropping to zero at the walls. The temperature distribution was also
flat in the central zone, was rising rapidly at the wall. The highest temperature occurs at the wall. The reason for these distributions was that the flow in the central region was faster than that near the wall. Since uniform heating was imposed on the basis of volume rather than mass flow rates, the fluid adjacent to the wall had more time to absorb more heat. Its temperature therefore was increased to higher values than the fluid in the central region. Buoyancy forces made the hottest fluid raise the fastest. Hence, the largest buoyancy forces were found adjacent to the wall. At the wall the velocity had to be zero (no slip boundary condition).

2. Velocity profile:

Figure 3 shows velocity profiles with buoyancy effect for guava juice, it has maximum value at the wall and low value at the centre of the pipe, the buoyancy force distort the velocity profiles and shift the maximum value of velocity from the center to near wall (high buoyancy effect value) and flattened till it exceed zero near the center of the heating cell Because the density and the viscosity of the fluids decrease with an increase of temperature near the region of the wall and then the velocity increase, so the region near the wall absorb low temperature due to the decrease in the residence time. And the velocity near the center fattened and here the residence time increase due to the decrease in the velocity, and this region absorb high amount of heat, so this may lead to temperature uniformity across the heating cell the. When buoyancy force is

considered this phenomenon is clearly observed and also it shows reverse flow. Figure 4 shows the velocity profiles without the buoyancy effect, the high velocity was observed near the center and low velocity near the wall.

3. Temperature profiles:

Temperature profiles show high values near the wall for both fluids and ohmic heating cells design. Figure 5 shows the temperature profiles with buoyancy effect of guava juice, it was observed that the temperature is high and uniform, because the buoyancy force distort the velocity profile and shift the high speed of flow to the wall, this significantly increase the temperature uniformity across the entire ohmic heating cell. Figure 6 shows the temperature profiles without the buoyancy effect for guava juice, low temperature across the heating cell and high near the wall was observed.

4. Current density:

Figure 7 shows high value of current density near the wall at the middle of the heating cell of guava juice with buoyancy effect, but when the buoyancy effect was not considered the current density was lower two times (see figure 8).

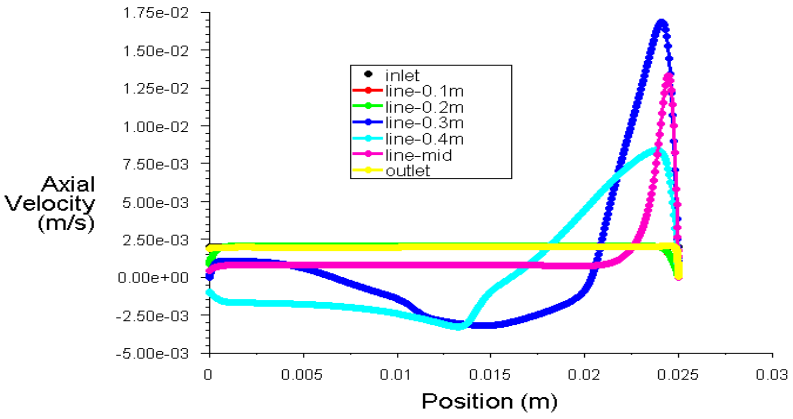

Figure 3 x-velocity of guava juice with buoyancy effect

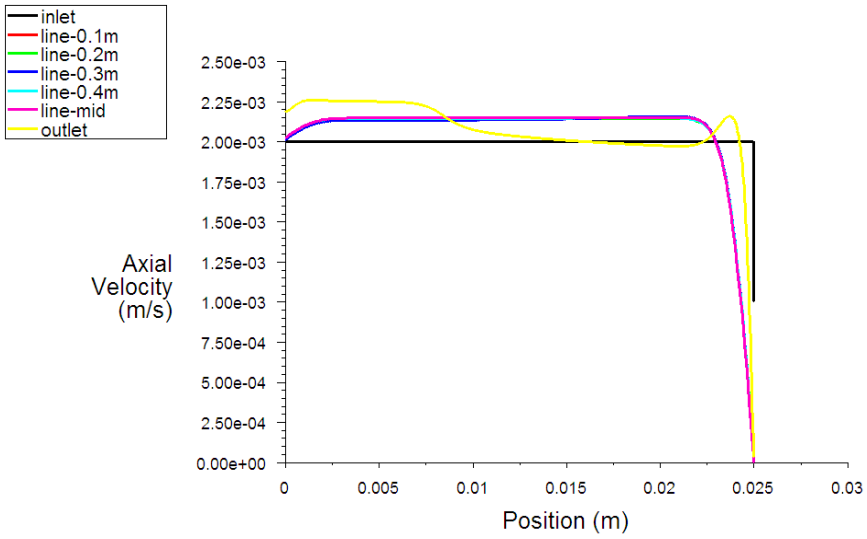

Figure 4 x-velocity profiles of guava juice without buoyancy effect

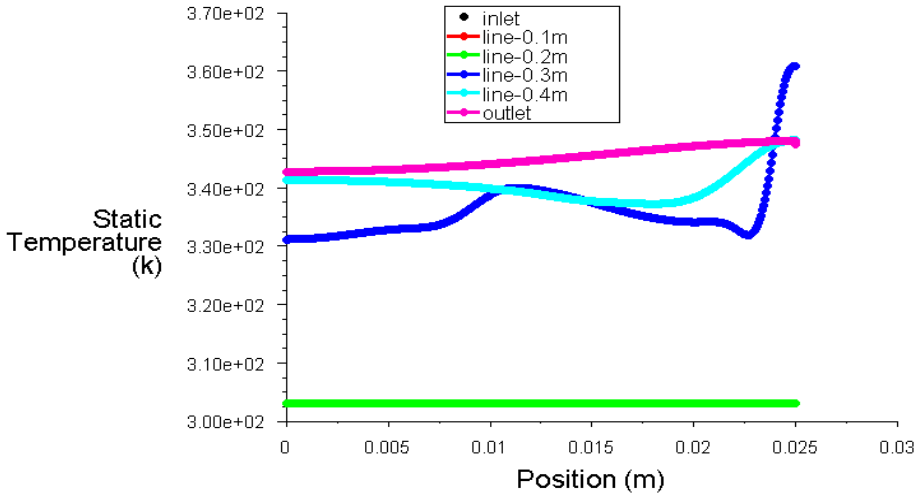

Figure 5 Temperature profiles of guava juice with buoyancy effect

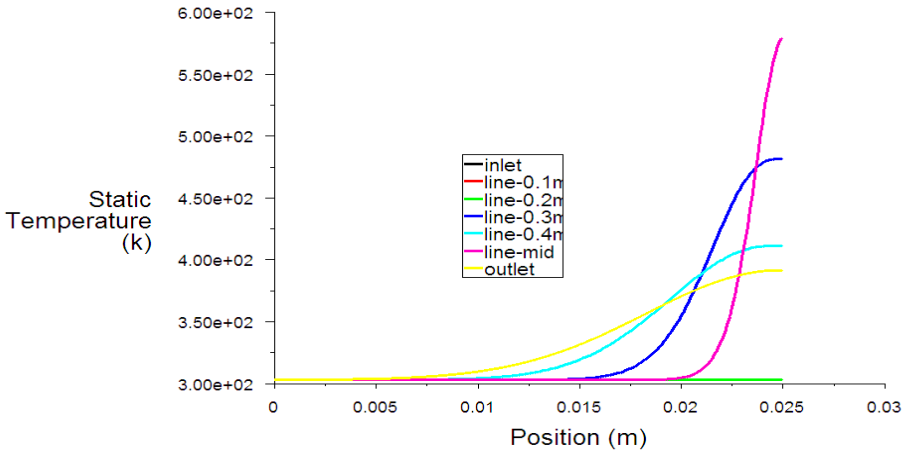

Figure 6 Temperature profiles of guava juice without buoyancy effect

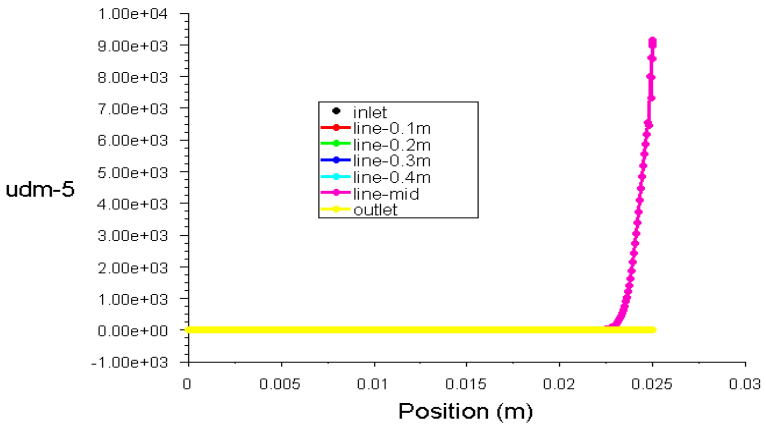

Figure 7 Current density (udm-5) of guava juice with buoyancy effect

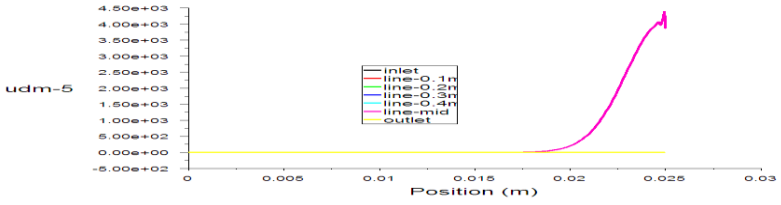

Figure 8 Current density (udm-5) of guava juice without buoyancy effect

2-The rectangular ohmic heating:

To test for justification of the flow results the numerical simulation was done for water flow on rectangular geometry and the input data for simulation was taken from published work of Ould El Moctar (1996) using CFD FLUENT. Figure 9 shows simulated velocity profiles with buoyancy effect at difference locations of the ohmic heating cell. The distortion of velocity profiles was clearly observed because of the buoyancy effect, it have high value near the wall and decrease gradually towards the center of the geometry. Figure 10 shows the velocity profiles at different location from the entrance without the consideration of buoyancy effect. It does not show any distortion, the high speed was near the center and low one near the walls and this will lead to non-uniformity in the temperature profiles. This suggested that the effect of buoyancy must be included in the CFD model to accurately describe the flow behavior. Figures (11 and 12) show comparison between predicted and experimental of the velocity profiles at the entrance and at the middle of the ohmic heating cell, respectively.

Good agreement was observed but some discrepancy was shown near the wall between the experimental and simulated result. The flow velocity is much higher at the middle of the channel than near the walls. The particles passing near the walls remain longer under the influence of the electric field and are heated more than those passing faster in the middle of the channel. This difference in residence time causes temperature gradient between the center of the flow and near the walls. The effect of buoyancy is an acceleration of the hot liquid near the wall. The consequence of this acceleration is that the velocity becomes more uniform through all the ohmic heating cell compared to the parabolic velocity at the inlet.
Figure 13 shows comparison of velocity profiles at the outlet of the fluid from the channel, the temperature shows strong effect on the velocity. The velocity near the wall exhibit high velocity, in the contrary to the inlet parabolic velocity.
Figure 14 show the importance of the buoyancy effect on the temperature profiles. The distortion of the velocity profiles transferred the high velocity from the center to near the wall which finally lead to change in residence time, the fluid near the hot wall receive less time to absorb heat and the fluid near the center receive more time and absorb more heat which finally lead to temperature uniformity across the entire of the channel. Figure 15 shows the temperature profiles without the buoyancy effect so the temperature is higher near the wall and lower towards the center, here the residence time have maximum value at the center and decrease gradually towards the walls, so the fluid near the wall receive more heat and near the center receive lower heat and this finally results in non uniformity of temperature profiles.

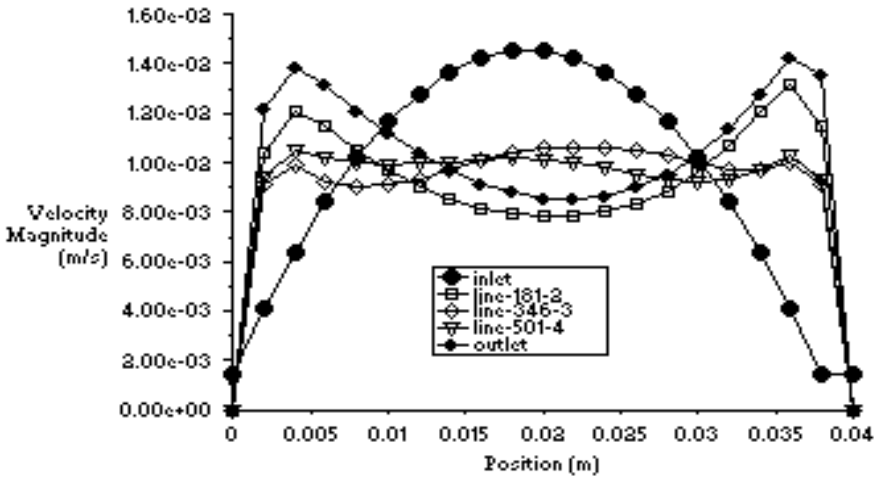

Figure 9 Simulated velocity profiles at difference locations of the System with buoyancy effect.

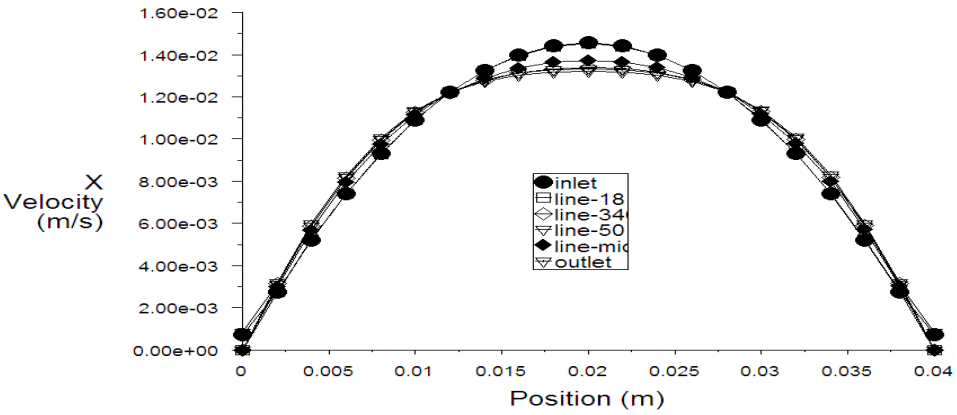

Figure 10 Simulated velocity profiles at different distances from the entrance to test section without buoyancy effect.

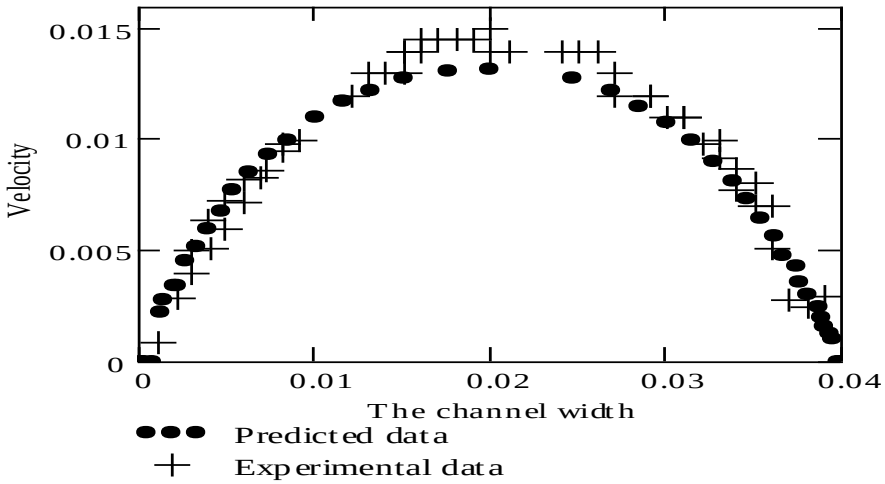

Figure 11 Comparison of predicted and experimental inlet velocity

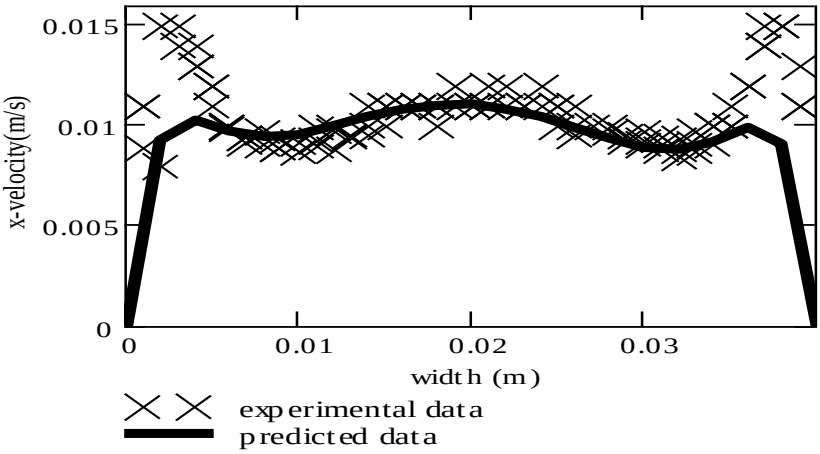

Figure 12 Comparison between predicted and experimental velocity profiles at the middle of the system.

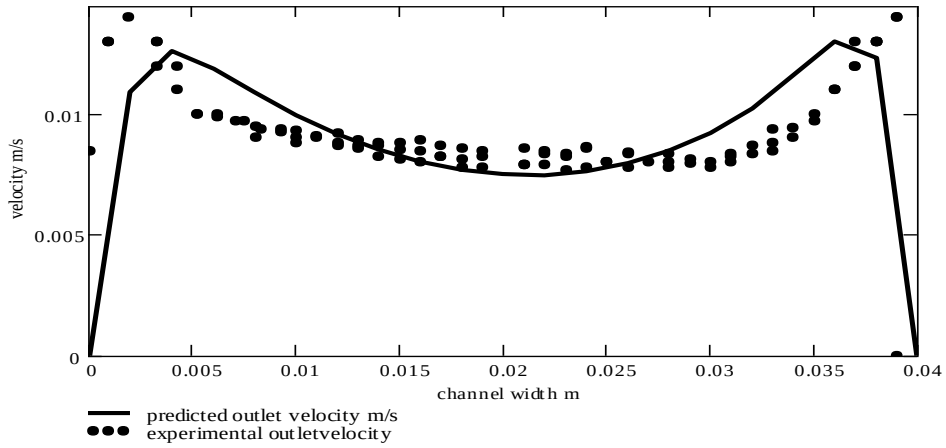

Figure 13 Comparison of experimental and predicted outlet velocity profiles.

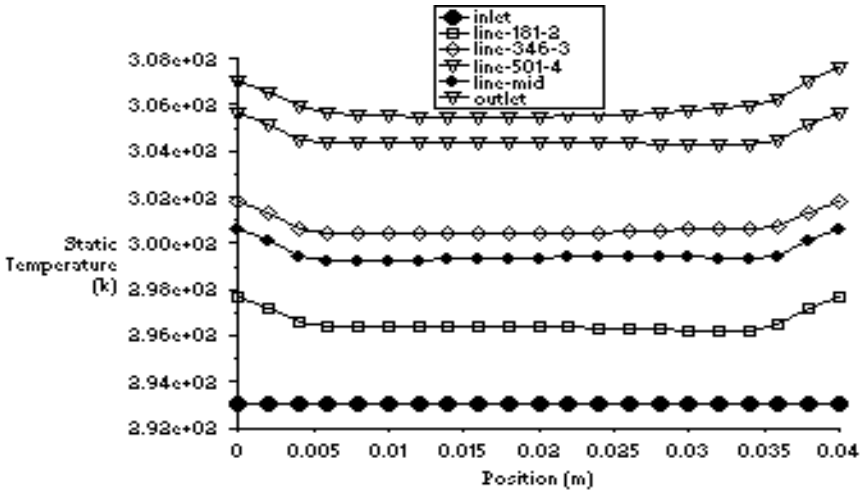

Figure 14 Temperature profiles at different distance from the entrance to test section with buoyancy effect.

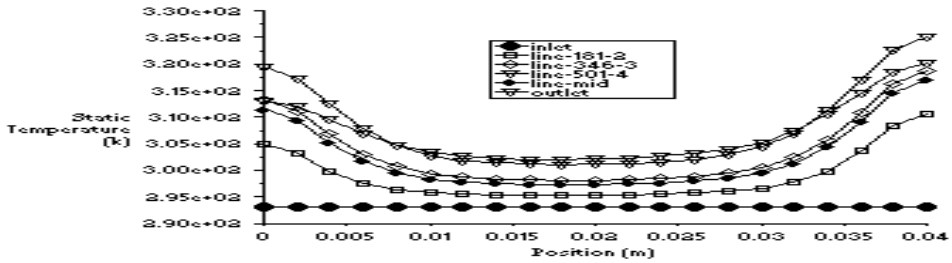

Figure 15 Temperature profiles at different distance from entranceto test section without buoyancy effect.

5. Conclusion:

1. A steady-state two-dimensional solution for this study was obtained using commercial, finite volumes method code FLUENT 6.1.The uniform structural grid was used to discretize the computational domain, the non-linear system of matrix equations arising from the finite volume method discretization was solved separately in sequentional manner using so called segregated solver.
2. The convergence criteria were given the residual of the solution less than 10^{-3} for momentum, continuity and 10^{-6} for energy and electric field.
3. The use of buoyancy has significant effects on the heating rate and temperature distributions and it may cause the reverse flow. It achieves reasonable current density near the electrode that was below the critical value 8000A/m^2 (Stirling, 1987).
4. The simulation show an increasing in the cross-sectional area of electrodes (ring electrode) is negligible. Also increasing the distance between electrodes had significant affect on ohmic heating.
5. The calculated velocity profiles for a channel flow were in good agreement with published literature.
6. The heating rate efficiency is higher in transverse (rectangular) electric field than the collinear ohmic heating (cylindrical).

Symbol	Description	Unit
A	Cross- sectional surface area of the electrodes	[m^2]
AC	Alternating current	[A]
b	The coefficient of temperature dependent Electrical conductivity	[$^0C^{-1}$]
C_p	Specific heat of liquid food	[J kg^{-1} $^0C^{-1}$]
D	Diameter of the heating cell	[m]
E	Voltage gradient or local electric field intensity	[Vm^{-1}]
g	Acceleration due to gravity	[m s^{-2}]
G_E	Acceleration due to electric field	[$G_E = E^{-2}$ bD^{-1}]
H	Height of the heating cell	[m]
I	Current	[A]
J	Current density	[A m^{-2}]
K	consistency index	[Pa s^n]
k	Thermal conductivity of liquid being heated	[w m^{-1} k^{-1}]
L_e	Distance between electrodes	[m]

Y	Rectangular diameter(width)	[m]
X	Half of rectangular width	[m]
(L/A)	Ratio of distance between electrodes to diameter of heating cell	
L	Electrode length	[m]
G	Volumetric flow rate	[m^3s^{-1}]
n	Flow behavior index	[dimensionless]
P	Pressure	[Pa]
Q	Volumetric heating generation	[w m^{-3}]
r	Radial position from center line	[m]
R	Resistance	[Ω]
T_{ref}	Reference temperature	[^{0}C]
t	Heating time	[sec]
T_{in}	Inlet fluid temperature	[^{0}C]
T	Temperature	[^{0}C]
V	Voltage	[volts]
v_m	Mean velocity	[ms^{-1}]
v_r	Radial velocity	[ms^{-1}]
v_z	Axial velocity	[ms^{-1}]
r	Radial coordinate	[m]
x	Axial coordinate	[m]

Dimensionless quantities

Gr_{pl}	Grashof number for power law fluid	[$g\rho^2\Delta T\beta R^{1+2n}v_m^{2-2n}K^{-2}$]
Gr	Grashof number,	[$g\ \rho^2\ \Delta T\ \beta\ D^3\mu^{-2}$]
Gr_{El}	Electrical Grashof number	[$E^2b\rho^2\Delta T\beta D^2\mu^{-2}$]
Re	Reynolds number	[$\rho v_m D\mu^{-1}$]

Greek symbols

ρ_{ref}	Reference density	[kg m^{-3}]
ρ	Density of liquid	[kg m^{-3}]
μ_a	Apparent viscosity	[Pa s]
τ	Shear stress	[Pa]
β	Thermal expansion coefficient	[$^0C^{-1}$]
α	Thermal diffusivity	[$k\ \rho^{-1}\ C_p^{-1}$]
γ	Shear rate	[s^{-1}]
σ	Electrical conductivity	[Sm^{-1}]
σ_0	Electrical conductivity of the fluid food at reference temperature	[Sm^{-1}]
ΔT	Difference between inlet and out let temperature	[^{0}C]
μ	Newtonian viscosity	[Pa s]

Subscripts

ref	Reference value

m	avaraged
El	electrical
out	outlet
e	Electrode
in	inlet
pl	Power law

REFERENCES

and experimental **Abdul Ghani, A. G., Farid, M. M., and Chen, X. D. (2002).** Theoretical Bacillus stearothermophilus in food pouches. investigation of the thermal inactivation of Engineering, 51, 221–228. Journal of Food

Barbosa- **Adrian, B. (1993).** Heat transfer (pp. 339–340). New York: Wiley.

Canovas, G. V., Gongora-Nieto, M. M., & Swanson, B.
G. (1998). Nonthermal electrical methods in food preservation.
Food Science and Technology International, 4(5), 363–370.

Bird, R. B., Stewart, W. E., & Lightfoot, E. N. (1976). *Transport phenomena* (Wiley International) New York: Wiley.

De Alwis, A. A. and Fryer, P. J. (1990a). The use of direct resistance
heating techniques in the food industry. *1. Food Eng.*, 11, 3-27.

Heating Process: **De Alwis, A.A.P. and Fryer, P.J. (1992).** Operability of the Ohmic 15:21-48. Electrical Conductivity Effects. *J. Food Eng*.

Kronig, R. & Ahsmann, G. (1949). The influence of an electric field on the convective heat transfer in Liquids. *Appl. Sci. Res. Sect. A, 2,3 l-2.*

Department of Food **Marcotte, M., (1999**). Ohmic heating of viscous liquid food, PhD thesis, University Mc Gill, Canada. Science and Agricultural Chemistry,

heating of **Ould El Moktar, A., Peerhossani, H., and Le Peurian, P. (1993).** Ohmic Transfer, 36 (12), 3143-3152. complex fluids. International Journal of heat and mass

verification of ohmic **YE, X., Ruan, R., Chen, P. and Doona, C. 2004**. Simulation and temperature mapping. Lebensmittel Wissenschaft heating in static heater using MRI Technologie. *37*, 49–58. und-